



Atmospheric mineral dust in dryland ecosystems: Applications of environmental magnetism

Richard L. Reynolds and Harland L. Goldstein

U.S. Geological Survey, MS 980, Box 25046, Denver, Colorado 80225, USA (rreynolds@usgs.gov)

Mark E. Miller

Southwest Biological Science Center, U.S. Geological Survey, 190 East Center Street, Kanab, Utah 84741, USA

Now at National Park Service, 2282 South West Resource Boulevard, Moab, Utah 84532, USA

[1] Magnetic properties of shallow (<10-cm depth), fine-grained surficial sediments contrast greatly with those of immediately underlying bedrock across much of the dry American Southwest. At 26 study sites in fine-grained (<63 μm) surficial sediments isolated from alluvial inputs, isothermal remanent magnetization (IRM; mean of 67 samples = $6.72 \times 10^{-3} \text{ Am}^2 \text{ kg}^{-1}$) is more than two orders of magnitude greater than that for underlying Paleozoic and Mesozoic sedimentary rocks. This contrast is mainly caused by the presence of silt-size, titanium-bearing magnetite particles in the surficial deposits and their absence in bedrock. Because of their size, composition, and isolated location, the magnetite particles represent a component of atmospheric dust likely deposited over the past few centuries. The positive correlation of sediment-IRM values with amounts of potential plant nutrients reveals the importance of atmospheric dust to soil fertility over much of the American Southwest. Subsequent disturbance of landscapes, by domestic livestock grazing as an example, commonly results in wind erosion, which then depletes exposed surfaces of original aeolian magnetite and associated fine-grained sediment. Declines in soil fertility and water-holding capacity in these settings can be estimated in some field settings via decreases in magnetic susceptibility, relative to nearby undisturbed areas. Along gentle hillslope gradients of the Colorado Plateau, field measures for aeolian magnetite demonstrate that the redistribution of deposited atmospheric dust influences landscape-level patterns in the distribution of invasive exotic plant species. Our results indicate that environmental magnetism has high potential for assessing the development and degradation of dry landscapes elsewhere.

Components: 11,600 words, 12 figures, 3 tables.

Keywords: mineral dust; magnetite; dry lands; soil fertility; invasive plant species; environmental magnetism.

Index Terms: 1512 Geomagnetism and Paleomagnetism: Environmental magnetism (1218); 1631 Global Change: Land/atmosphere interactions (1218); 1625 Global Change: Geomorphology and weathering (0790).

Received 23 February 2010; **Revised** 21 May 2010; **Accepted** 28 May 2010; **Published** 17 July 2010.

Reynolds, R. L., H. L. Goldstein, and M. E. Miller (2010), Atmospheric mineral dust in dryland ecosystems: Applications of environmental magnetism, *Geochem. Geophys. Geosyst.*, 11, Q07009, doi:10.1029/2010GC003103.

1. Introduction

[2] Concerns about ongoing and future changes in the physical and biotic compositions of dryland ecosystems drive current interest to understand the recent development and contemporary vulnerability of these ecosystems, as well as the geological materials that support them. Despite their generally barren appearance, dry lands may harbor high levels of soil fertility, which supports a high degree of biodiversity, and these regions contribute in many ways to national, regional, and local economies. Dry landscapes are particularly sensitive to environmental change because they consist of widespread surface exposures of lithogenic substrates (rock-derived soil and surficial deposits) with sparse vegetation, rendering these surfaces vulnerable to erosion by wind and water. Dryland areas contribute a disproportionate fraction of global airborne dust that can affect climate, soil fertility in far-distant ecosystems, melting rates of ice and snow, as well as human health and infrastructure.

[3] This paper addresses topics in deposited dust, contemporary surficial processes, and current nutrient status of dryland ecosystems from environmental magnetic investigations of upland soil and surficial deposits in the American Southwest. New data are combined with previously published results to (1) identify regional spatial patterns in mineral dust deposited on mostly sandy dryland surfaces that has been recently deposited across landscapes and redistributed by geomorphic processes, (2) elucidate the influence of such dust on current ecosystem fertility, and (3) recognize losses in dust and related soil fertility caused by human disturbances of landscapes within the past approximately 150 years. Finally, this paper presents examples about how simple magnetic susceptibility field measurements can be applied to assess soil fertility on the basis of ongoing gains (dust deposition) or losses (wind erosion) of aeolian magnetite, under conditions where the magnetite is associated with potential plant nutrients. The magnetic results further yield insight into contemporary soil-geomorphic relations that may promote the deleterious spread of invasive grasses within dry lands.

[4] Some of the first research in environmental magnetism investigated erosion and sediment transport by wind [Thompson and Oldfield, 1986; Evans and Heller, 2003]. Applications of environmental magnetism to aeolian processes and deposits have covered an enormous range of spe-

cific topics that include records of past climate change from deposited dust in terrestrial and marine settings, linkage of airborne metal pollution with anthropogenic sources, and characterization of Fe oxide mineralogy in modern and Quaternary dust [e.g., Bloemendal and deMenocal, 1989; Maher and Thompson, 1999; Liu et al., 2007; Lázaro et al., 2008; Maher, 2009]. Many environmental magnetic investigations of contemporary dry landscapes have been motivated to understand the influence of precipitation on the origins of iron oxide minerals in thick loess deposits with application to paleoclimatic interpretations [Maher et al., 2003; Maher, 2009]. Other environmental magnetic studies have probed possible desert sources of dust that formed the thick Asian loess deposits [Maher et al., 2009]. Magnetic study of source-region soils has also been conducted to characterize lithogenic dust from the Asian mainland so that anthropogenic aerosolic pollutants could be recognized in dust fall onto South Korea [Kim et al., 2005]. Several environmental magnetic studies have examined aeolian processes responsible for the development of dry landscapes, in particular bearing on sources of sand and the distribution of dunes [e.g., Walden et al., 2000; Newsome and Walden, 2000; Muhs et al., 2003]. Very few environmental magnetic studies, however, have examined the roles of airborne mineral dust in the recent development and wind-erosion degradation of dry landscapes under natural and human influences.

2. Settings and Methods

[5] We examine herein upland (non-riparian) settings in arid and semi-arid regions of the western United States, with focus on the Colorado Plateau (Figure 1). The settings in the Colorado Plateau are dominantly underlain by Permian to Jurassic sandstone, siltstone, and limestone and are typical of most of the Colorado Plateau [Huntoon et al., 1982; Billingsley et al., 2002]. The surficial deposits described here lie directly on sedimentary rocks that lack magnetite, except as rare inclusions in quartz grains [Reynolds et al., 2001a]. Magnetite-bearing igneous rocks occupy only small areas of the central Plateau (see Figure 1). The western and southwestern margins are covered by Tertiary lavas, dominantly basaltic. In contrast, geologic-physiographic provinces surrounding the Plateau to its west and southwest (generally the upwind direction) contain large desert areas of felsic (silicic) igneous rocks [Reed et al., 2005].

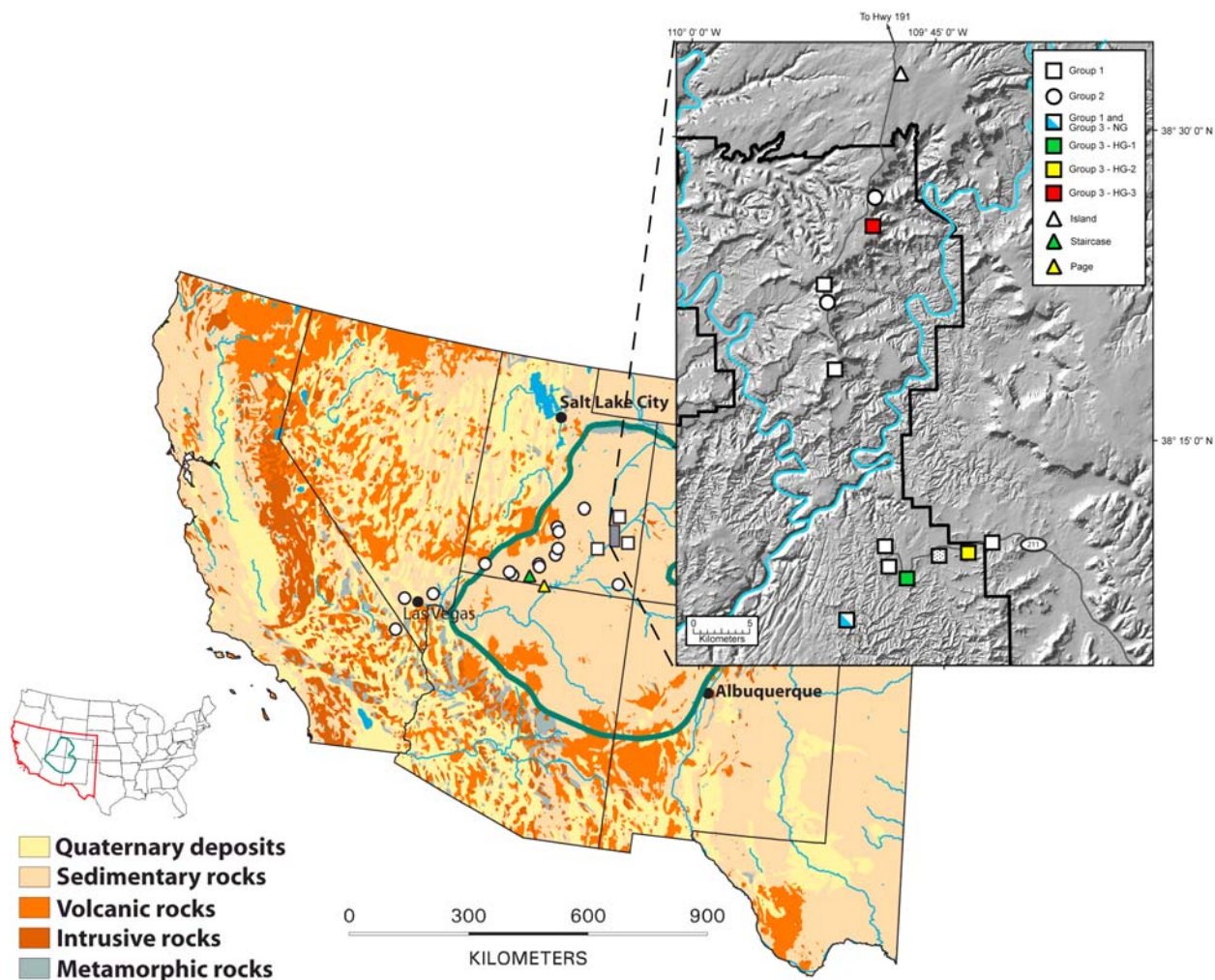


Figure 1. Generalized geologic map of the southwestern United States showing locations of sampling sites. Site 8U-5 is indicated by stippled square in the inset map. Green line denotes outline of the Colorado Plateau.

[6] Surficial deposits at two types of settings (Figure 1 and Table 1) were sampled for laboratory measurement. One type of setting (represented by sample groups 1 and 2 (Table 1)) included sediment-filled depressions on mesa tops and slickrock buttes formed on mostly flat-lying sedimentary rocks (Figure 2). These settings were chosen because they consist of surfaces isolated from alluvial and colluvial sedimentation and, thus, fine-grained sediment at these sites might contain aeolian dust.

[7] At each of these group-1 and -2 sites, the sediment was covered by biologic soil crusts (BSC). Biologic soil crusts are important components in many deserts, because they protect surface materials from erosion, absorb water, promote water infiltration, and add atmospheric nitrogen and carbon to soils [Belnap and Gillette, 1998;

Belnap and Lange, 2003]. The BSC also traps dust because of its roughness and its ability to bind particles within a cyanobacterially produced network of interlocking filaments. Isolated sites were selected to represent surfaces that had never been disturbed by human activity, with the exception of site 8U-5, which had been grazed by domestic livestock until 1975. Group 1 sites are clustered in the central Colorado Plateau and have been previously examined for properties of bulk sediment (<2-mm fraction) [Reynolds *et al.*, 2001a]. Group 2 sites provide spatial coverage across the Colorado Plateau, extending from the eastern edge of the Mojave Desert on the west to southeastern Utah on the east. Goldstein *et al.* [2008] have reported on the fine-fraction (<63 μm) sediments at these sites.

[8] The second type of setting consists of grasslands and shrublands on gentle slopes, not greater

Table 1. Studies That Used Environmental Magnetic Methods for Investigations of Dryland Ecosystem Dynamics^a

Settings	Locations	Group	N	Size	Magnetic Methods	Other Methods	Reference
Isolated surfaces	Colorado Plateau	1	151	<2 mm <63 μm	IRM, HIRM, FDMS, petrog	Chem-XRF, -ICP; X; carb; PSD; RN	<i>Reynolds et al.</i> [2001a] and this study
Isolated surfaces	Mojave Desert to Colorado Plateau	2	67	<63 μm	IRM, HIRM, petrog	Chem-ICP; X; carb; PSD; RN; Pb isot.; Sr isot.	<i>Goldstein et al.</i> [2008] and this study
Shallow hillslopes; Dust traps	Colorado Plateau	3	74	<2 mm <63 μm <53 μm	IRM, MS, petrog	Chem-ICP; X; carb; PSD; Sr isot.	<i>Reheis</i> [2003], <i>Goldstein et al.</i> [2005], <i>Reynolds et al.</i> [2006a], and this study
Shallow hillslopes	Colorado Plateau	3/4	938	<2 mm <63 μm	IRM, HIRM, MS, ARM, petrog	Chem-ICP; X; carb; PSD	<i>Goldstein et al.</i> [2005] and <i>Reynolds et al.</i> [2006c]
Shallow hillslopes; Dust traps	Colorado Plateau	3/4	480	<2 mm <63 μm <53 μm	IRM, petrog	Chem-ICP, X; carb; PSD; Sr isot.; OSL; soil	<i>Reheis et al.</i> [2005]
Shallow hillslopes	Colorado Plateau		214	Bulk sediment	Field MS	Plant community composition	this study and M. E. Miller (unpublished data, 2009)
Shallow hillslopes	Colorado Plateau		17	<2 mm	IRM, HIRM, MS	Chem (multiple methods, see ref.); carb; PSD; CEC	<i>Miller et al.</i> [2006]
Shallow hillslopes	Colorado Plateau		430	<2 mm	MS	Chem-ICP; carb; PSD; CEC; C + N;	<i>Fernandez et al.</i> [2008]
Shallow hillslopes	Colorado Plateau		61	<2 mm	IRM	Chem-ICP; carb; PSD; C + N; ρ ; CO ₂	<i>Neff et al.</i> [2005]
Isolated surfaces; Dust traps	Mojave Desert		70	<53 μm	IRM, HIRM, MS, FDMS, ARM, petrog	Chem-ICP, -INAA; PSD	<i>Reheis et al.</i> [2009]
Isolated surfaces	Mojave Desert		20	<63 μm	IRM, HIRM, MS, ARM, petrog	Chem-XRF, -ICP; X; carb; PSD	<i>Reynolds et al.</i> [2006b]

^aIsolated surfaces, sites that are isolated from alluvial or colluvial influx of sediment, including mesa tops, small depressions in bedrock (potholes), and flat grassland surfaces remote from bedrock. Shallow hillslopes, primarily grassland or shrubland sites on gently sloping surfaces that can receive locally derived detritus from nearby bedrock outcrops. "Group" refers to sample groups described in text; groups 3/4 are from the same study areas; group 3 represents 0–10-cm depths of samples; group 4 represents depths >10 cm and are not discussed herein. N, number of samples used for magnetic analysis and number of field measurements by Miller (this study). Size, sieved particle sizes of samples used for magnetic property measurements. Magnetic methods: IRM, isothermal remanent magnetization; HIRM "hard" IRM; MS, magnetic susceptibility; FDMS, frequency-dependent MS; ARM, anhysteretic RM; petrog, reflected light microscopy. Other methods: Chem-XRF, Chem-ICP, Chem-INAA, chemical analyses by X-ray fluorescence, inductively coupled plasma, and instrumental neutron activation analysis methods, respectively; X; X-ray diffraction to identify mineralogy; carb, measurement of calcium carbonate concentration by Chittick method; PSD, particle-size determination by laser-diffraction method [*Goldstein et al.*, 2008]; CEC, cation exchange capacity including exchangeable cation concentrations; C + N, measurement of carbon (total soil C and chloroform-labile C) and soil nitrogen; ρ , bulk density; CO₂, carbon dioxide soil flux; RN, measurement of concentration of Cesium-137; Pb isot., stable lead isotope (for isotopes 204, 206, 207, 208); Sr isot., ⁸⁶Sr and ⁸⁷Sr isotopy. OSL, optically stimulated luminescence dating. Soil, field descriptions of soil properties.

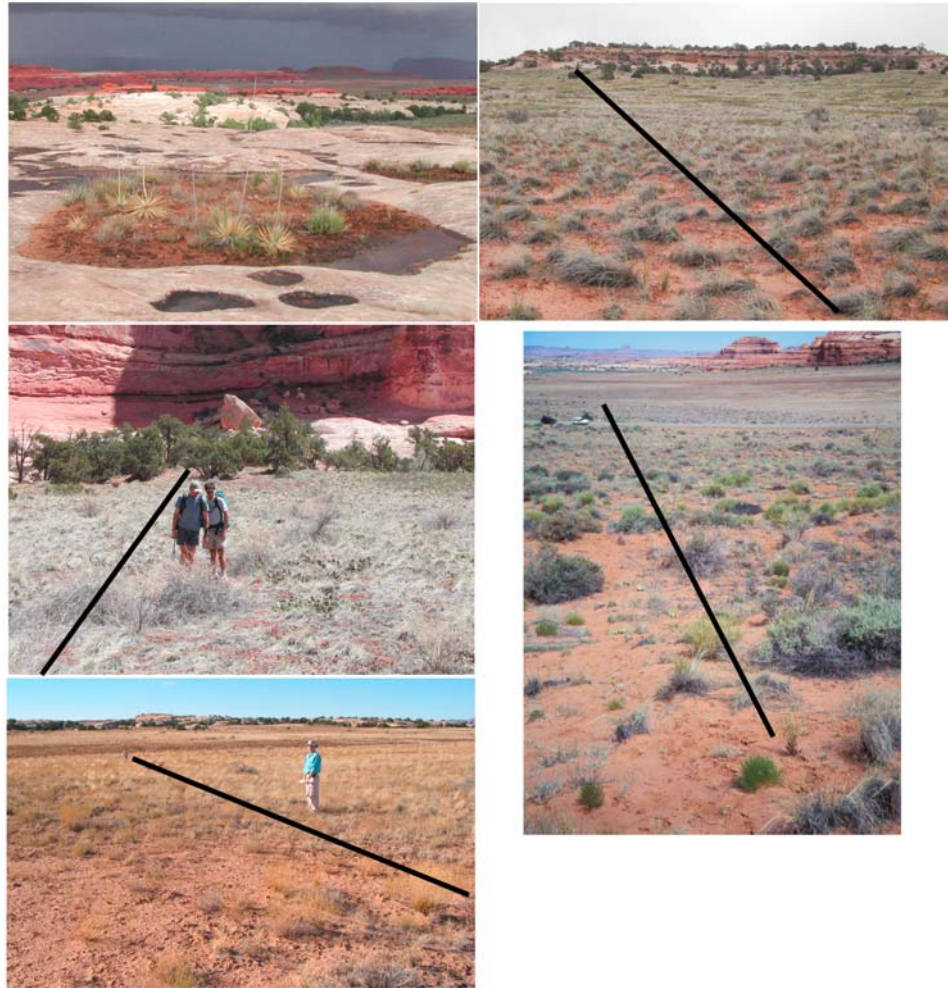


Figure 2. Photographs showing field sites. (top left) Sediment-filled depression characteristic of group-1 and -2 sites; (middle left) site NG, line indicating location of transect, people standing near position 8 (Figure 7a); (bottom left) site HG-1, line indicating location of transect, person in foreground near position 2 and downslope end of the line near position 6 (Figure 7b); (bottom right) site HG-2, line indicating location of transect looking downslope (Figure 7c); and (top right) site HG-3, line indicating position of transect looking up slope (Figure 7d).

than 3–4° (Figure 2). This setting was chosen for investigation to elucidate downslope changes in soil properties and how these properties influenced plant community composition, including the distribution of exotic species such as *Bromus tectorum* (cheatgrass). Surficial sediments at these settings (group 3 (Table 1)) are sands, loamy sands, and sandy loams, having been derived mainly from sandstones in the headwalls above the slopes. One grassland site has remained undisturbed (never-grazed (NG) site [Reynolds et al., 2006a]). The BSC on the NG surface is well established in a mature association of lichens, mosses, and cyanobacteria. Three other grassland surfaces in Canyonlands National Park (CNP) were previously used for livestock grazing until the mid-1970s, when livestock use ceased in the Park. The his-

torically grazed grasslands at sites HG-1 and HG-2 [Neff et al., 2005; Reynolds et al., 2006a] are surrounded by Permian Cedar Mesa Sandstone as is the NG grassland. The previously grazed grassland at Grays Pasture (HG-3) is formed on Jurassic Navajo Sandstone, as is another grassland (Island, 1869-m elevation) located north of HG-3 on lands that are currently grazed. In addition to this pair of grasslands on Navajo Sandstone soils, comparisons of formerly and currently grazed areas were made at two shrubland sites. One shrubland site (Staircase, 1940-m elevation) also is on soils derived from Navajo Sandstone, whereas the second shrubland site (Page, 1227-m elevation) is on soils formed from Jurassic Entrada Sandstone. At the Staircase site, livestock have been excluded from a 0.3-ha study area that was fenced off in 1967. At



the Page site, livestock have been excluded from lands adjacent to a highway by a fence constructed in the late 1960s.

[9] Although natural factors and processes over at least 40,000 years have produced a variety of surficial deposits and paleosols in the study region [Reheis *et al.*, 2005; Reynolds *et al.*, 2006b], we report here on sediment samples and field measurements collected within the upper 10 cm of the surface. This shallow depth interval exerts fundamental controls on ecosystem dynamics (principally on establishment and growth of herbaceous plants, and on the capture and retention of soil resources) and records important differences bearing on landscape stability and vulnerability to change across the study region.

[10] The ages of the sampled deposits are difficult to determine precisely. Group 1 and 2 samples typically consist of three depth intervals in a deposit (0–1 cm, 1–2 cm, and 2–5 cm). The top sample was taken from mature BSC (a community of cyanobacteria, lichen, and moss) that is estimated to represent accumulated sediment over about 100 years [Belnap and Lange, 2003], with the exception of site 8U-5 that lacked lichen and moss. Sediment mixing within some deposits related to bioturbation is expected [Reynolds *et al.*, 2001a]. Group 3 samples were taken in the 0–10-cm-depth interval that included BSC, where present. In the undisturbed site (NG), the BSC was well developed, but in disturbed settings, the BSC was immature and weakly developed, or absent. The shallow, young, and almost constantly dry sediment (except following rare precipitation events) at all settings shows no evidence of mineral alteration related to soil formation.

[11] This report presents two types of data: (1) laboratory data on samples from surficial deposits and bedrock, and (2) data from field measurements. In the laboratory, magnetic measurements were made on bulk sediment dried in air and rock fragments placed securely into 3.2-cm³ plastic cubes and normalized for sample mass. Earlier reports interpreted magnetic, chemical, textural, results on more than 1600 returned samples [Reynolds *et al.*, 2001a, 2006a; Neff *et al.*, 2005; Goldstein *et al.*, 2005, 2008; Miller *et al.*, 2006; Fernandez *et al.*, 2008]. In this article, new results on group-1 samples are reported for the <63- μ m fraction (silt and clay, or fines) and for group-2 samples for bulk sediment (<2-mm fraction). Data on samples (<2-mm fraction) from grassland hillslope sites NG and HG-1 have been reported previously [Reynolds *et al.*,

2006a], and new results from hillslope sites HG-2 and HG-3 are presented here. None of the field measurements reported here have been previously presented.

[12] Magnetic susceptibility (MS) was determined in the laboratory in a 0.1 milliTesla induction at frequencies of 600 Hz and 6,000 Hz, using a Sapphire Instruments susceptometer with a sensitivity better than $2 \times 10^{-9} \text{ m}^3 \text{ kg}^{-1}$. As a test for ultra fine-grained pedogenic magnetization carried by superparamagnetic (SP) grains, frequency dependence of MS (FDMS) was defined as $(\text{MS}_{600 \text{ Hz}} - \text{MS}_{6000 \text{ Hz}})/\text{MS}_{600 \text{ Hz}} \times 100$. Isothermal remanent magnetization (IRM) was acquired after exposing a sample to a strong magnetic field, first at 1.2 Tesla (T) and then at a backfield of 0.3T. Remanence was measured using an Agico JR-5A (90-Hz) spinner magnetometer with a sensitivity of about 10^{-5} A m^{-1} . Hard IRM (HIRM) was calculated as $(\text{IRM}_{1.2\text{T}} - \text{IRM}_{0.3\text{T}})/2$ and the S parameter as $\text{IRM}_{0.3\text{T}}/\text{IRM}_{1.2\text{T}}$. High S values (to a maximum value of 1) indicate large amounts of magnetite relative to hematite, and decreasing values indicate increasing amounts of hematite.

[13] Reflected-light microscopy complements our magnetic measurements by helping to determine the types, amounts, and grain sizes of magnetic minerals. In this way, reliable identification of different Fe-Ti oxide minerals can be made on grains larger than about 3 μm in diameter, and the presence of iron oxide can be discerned from grains as small as about 1–2 μm . The grains were prepared as polished grain mounts after isolation from the bulk sediment in a pumped-slurry magnetic separator [Reynolds *et al.*, 2001b].

[14] From the beginning, this research was partly intended to develop tools for field investigations of surficial soil properties in relation to land use and the spatial distribution of invasive plant species. At the outset of our studies on dryland ecosystems of the Colorado Plateau, field measurement of magnetic susceptibility revealed differences between bedrock units and their overlying soil and surficial deposits. Subsequent laboratory-based investigation to examine the reasons for these discrepancies has recently allowed us to use field-based measurements of MS to characterize rapidly the magnetic properties of dryland surficial deposits and to improve our understanding of the conditions, causes, and consequences of variations in magnetic mineralogy in specific dryland settings. At the NG site, field measurements of MS were taken at systematic 5- or 10-m intervals along 20–40 m transects

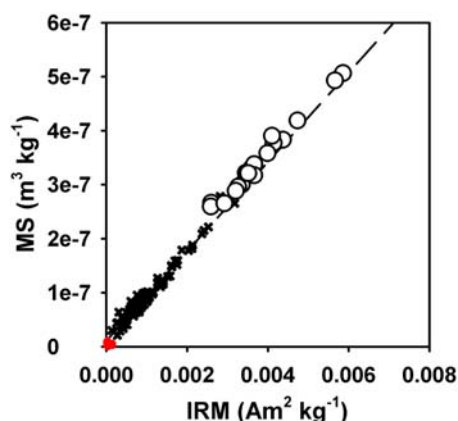


Figure 3. Plot of magnetic susceptibility against isothermal remanent magnetization for group-1 sediments (cross, bulk samples; open symbols, samples composed of silt and clay) and associated bedrock ($n = 14$; clustered red symbols).

located in permanently marked plots where dynamics of the invasive exotic annual grass *Bromus tectorum* have been studied since 1996 [Belnap and Phillips, 2001]. Plots at this site differ from each other with respect to their geomorphic setting and slope position. At the Island, Staircase, and Page sites, MS measurements were taken at systematic five-pace intervals along transects that traversed 0.25–0.5 ha within paired formerly and currently grazed areas. Sampling at each of these three sites was conducted on gentle ($<3^\circ$) backslopes in similar geomorphic settings. The field-based MS instrument was a model SM-20 from ZH Instruments, having a sensitivity of 1×10^{-6} SI units, that senses depths less than 10 cm below the surface.

3. Results and Interpretations: Dust Concentrations and Dust-Fertility Relations

3.1. Magnetic Properties of Sediments in Isolated Settings

[15] The magnetic properties of sediments on isolated dry landscape surfaces differ greatly from their underlying bedrock where examined over the Mojave Desert, Great Basin Desert, and Colorado Plateau of western United States (70 sites [Reynolds *et al.*, 2001a, 2006c; Goldstein *et al.*, 2005, 2008; H. Goldstein and R. Reynolds, unpublished data, 2008]). For group-1 sites, values of highly correlated ($R^2 = 0.96$) bulk-sediment MS and IRM are much greater than the MS and IRM values of associated underlying bedrock (Figure 3).

At individual sites, bulk-sediment IRM values are typically larger than those of the associated bedrock by a factor >20 . The fine-fraction samples in group 1 have significantly higher values of strongly correlated MS and IRM ($R^2 = 0.98$ (Figure 3)) than do the corresponding bulk-sediment samples ($R^2 = 0.96$), indicating that magnetic minerals are preferentially concentrated in the fines. Strongly correlated ($R^2 = 0.98$) values of MS and IRM for group-2 samples (fines from isolated surfaces from eastern California onto the Colorado Plateau) are also much higher than corresponding values for bulk sediment and underlying bedrock [Goldstein *et al.*, 2008].

[16] Other contrasts and similarities among surficial deposits are further revealed when groups 1 and 2 are recast within particle-size classes by regional location (Mojave Desert and Colorado Plateau) (Figure 4). The fine-fraction sediment has significantly higher ($P < 0.001$) MS, IRM, and HIRM values compared with bulk sediment for each of the depth categories and with associated bedrock (Figures 4a–4c and Table 2). With respect to the S parameter (Figure 4d), values for fine and bulk fractions from both regions are high relative to associated underlying rock. Such differences are magnified when comparing S values in fine sediments with those of underlying rock having sufficient hematite concentrations to impart red hues to the rock (Figure 5). Other comparisons among S-parameter results indicate the following: (1) for Mojave fines, mean S (0.86; standard deviation, 0.06; $N = 15$) is significantly greater ($P = 0.016$) than mean S for Colorado Plateau fines (0.79; standard deviation, 0.09; $N = 47$); and (2) fine and bulk fractions of the Mojave samples are not significantly different, but Colorado Plateau fines have significantly higher S than corresponding bulk samples (Figure 4d and Table 2).

[17] On the basis of petrographic examination, magnetic minerals in surficial sediments consist mainly of strongly magnetic magnetite and titanomagnetite (typically $\sim 4\text{--}20 \mu\text{m}$), commonly intergrown with hematite, ilmenite, pseudobrookite, and ilmenorutile. Such Fe-Ti oxide minerals, which formed originally in igneous rocks during initial cooling [Haggerty, 1976], are absent in the associated bedrock units. The association of magnetite and Ti is indicated by increasing Ti with increasing IRM (Figure 6). Spherical, silt-size ($<20 \mu\text{m}$) magnetic particles are also found rarely and exclusively in sediments of the biologic soil crust. The spherical particles mostly consist of magnetite and silicates in metallographic textures that are

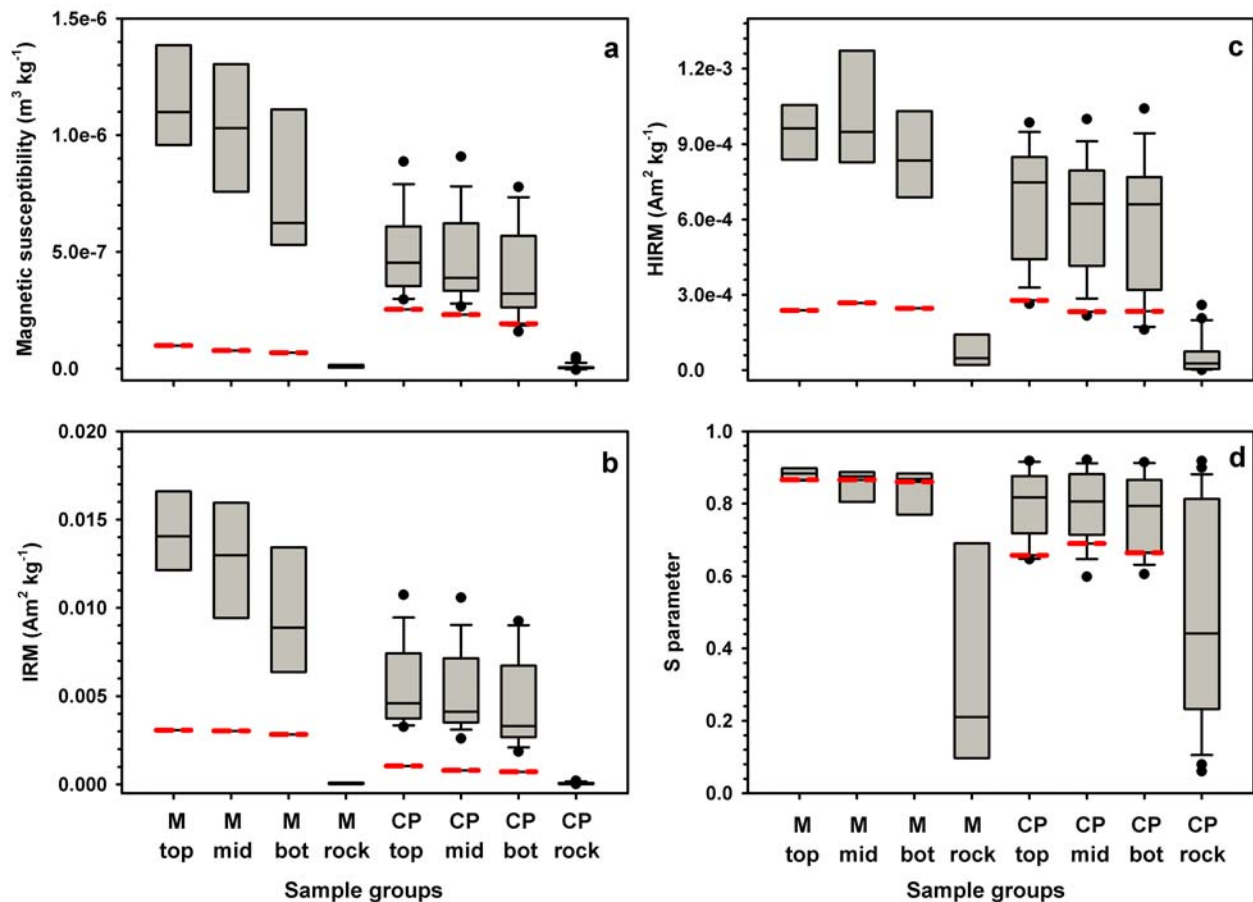


Figure 4. Box plots of magnetic properties of sediment and associated rock from sites in the Mojave Desert (M) and on the Colorado Plateau (CP). Combined samples denoted as top, uppermost sediment samples at each site, 0–1 cm; mid, middle samples, 1–2 cm; bot, bottom samples, typically 2–5 cm; rock, bedrock samples. The silt-plus-clay fraction is represented by boxes; the median values for the bulk sediments are represented by red lines. The lower (upper) boundary of each box indicates the 25th (75th) percentile; line within a box indicates median. Error bars above (below) the box indicate the 90th (10th) percentiles. Insufficient data ($n < 9$) precluded plotting 10th and 90th percentiles for the Mojave Desert sites.

identical to textures in magnetic fly ash particles [Locke and Bertine, 1986]. Some hematite in the surficial sediments appears to have been reworked from bedrock, such as large (80–160 μm) specular hematite that formed diagenetically in red beds.

3.2. Magnetic Evidence for Far-Traveled Dust

[18] The silt-size magnetite and titanomagnetite in the surface sediments that are absent in nearby sedimentary rocks are the only observed mineralogic sources for the large differences in magnetic properties between sediments and rock. Relations between magnetite (indicated by IRM and MS values) and Ti concentrations are consistent with petrographic observations of ubiquitous titaniferous magnetite in these sediments. The presence of these

strongly magnetic minerals in topographically isolated settings can be explained only as windborne dust. The presence of fly ash magnetite is further evidence for aeolian input [e.g., Hunt, 1986]; these particles were likely produced at coal-burning power plants, which are >100 km from most sampling sites. The higher S parameter values for sediments vis-à-vis hematite-bearing rocks also reflect the airborne addition of detrital magnetite. Petrographic observations and S-value data indicate that some hematite is added as dust to these landscapes and that some proportion of HIRM in sediments atop red beds is directly inherited from the bedrock.

[19] The magnetic evidence for aeolian dust in these settings is corroborated by results from geochemical, particle-size, and X-ray diffraction



Table 2. Summary of Magnetic Data and Statistical Analysis for Sediment Samples From Isolated Settings, Grouped by Location^a

ColoPla						Mojave					
Sample	N	Mean	Standard Error	Median	Significance	Sample	N	Mean	Standard Error	Median	Significance
MS top f	17	4.96E-07	4.25E-08	4.53E-07	a	MS top f	5	1.16E-06	9.86E-08	1.10E-06	a
MS mid f	16	4.71E-07	4.64E-08	3.88E-07	a	MS mid f	5	1.03E-06	1.26E-07	1.03E-06	a
MS bot f	15	3.95E-07	5.32E-08	3.21E-07	a	MS bot f	5	7.81E-07	1.39E-07	6.25E-07	a
MS top b	56	1.07E-07	6.45E-09	9.90E-08	b	MS top b	5	3.07E-07	5.81E-08	2.54E-07	b
MS mid b	34	8.77E-08	7.38E-09	7.76E-08	c	MS mid b	5	2.85E-07	6.79E-08	2.31E-07	b
MS bot b	31	8.34E-08	8.95E-09	6.81E-08	c	MS bot b	5	2.25E-07	6.06E-08	1.92E-07	b
MS rocks	26	6.63E-09	2.48E-09	3.47E-09	d	MS rocks	5	9.22E-09	3.67E-09	6.53E-09	c
IRM top f	17	5.66E-03	5.49E-04	4.59E-03	a	IRM top f	5	1.43E-02	1.01E-03	1.41E-02	a
IRM mid f	16	5.28E-03	5.74E-04	4.12E-03	a, b	IRM mid f	5	1.28E-02	1.63E-03	1.30E-02	a, b
IRM bot f	15	4.44E-03	7.02E-04	3.31E-03	b	IRM bot f	5	9.69E-03	1.65E-03	8.88E-03	b
IRM top b	56	1.19E-03	7.73E-05	1.05E-03	c	IRM top b	5	3.69E-03	6.76E-04	3.07E-03	c
IRM mid b	34	9.34E-04	9.16E-05	7.97E-04	d	IRM mid b	5	3.39E-03	8.16E-04	3.03E-03	c
IRM bot b	31	8.56E-04	1.10E-04	7.20E-04	d	IRM bot b	5	2.84E-03	7.72E-04	2.83E-03	c
IRM rocks	31	6.80E-05	1.12E-05	5.67E-05	e	IRM rocks	5	5.39E-05	1.62E-05	5.66E-05	d
HIRM top f	17	6.58E-04	5.56E-05	7.47E-04	a	HIRM top f	5	9.50E-04	5.65E-05	9.62E-04	a
HIRM mid f	16	6.20E-04	5.62E-05	6.63E-04	a	HIRM mid f	5	1.03E-03	1.03E-04	9.49E-04	a
HIRM bot f	16	5.79E-04	7.26E-05	6.61E-04	a	HIRM bot f	5	8.54E-04	8.91E-05	8.35E-04	a
HIRM top b	56	2.85E-04	1.79E-05	2.78E-04	b	HIRM top b	5	2.83E-04	6.72E-05	2.38E-04	b
HIRM mid b	34	2.51E-04	2.55E-05	2.34E-04	b	HIRM mid b	5	3.29E-04	8.37E-05	2.68E-04	b
HIRM bot b	31	2.40E-04	2.89E-05	2.35E-04	b	HIRM bot b	5	2.45E-04	7.50E-05	2.46E-04	b
HIRM rocks	26	5.75E-05	1.48E-05	2.65E-05	c	HIRM rocks	5	7.48E-05	3.03E-05	4.77E-05	c
S top f	17	0.80	0.02	0.82	a	S top f	5	0.88	0.01	0.88	a
S mid f	16	0.79	0.02	0.81	a	S mid f	5	0.85	0.03	0.88	a
S bot f	16	0.78	0.03	0.79	a	S bot f	5	0.84	0.04	0.87	a
S top b	56	0.67	0.02	0.66	b	S top b	5	0.87	0.01	0.86	a
S mid b	34	0.66	0.03	0.69	b	S mid b	5	0.83	0.04	0.87	a
S bot b	31	0.64	0.04	0.66	b	S bot b	5	0.83	0.07	0.85	a
S rocks	25	0.49	0.06	0.44	c	S rocks	5	0.36	0.15	0.21	b

^aColoPla, Colorado Plateau samples; Mojave, Mojave Desert samples; N, number of samples; top, mid, bot refer to sample depths: 0–1 cm, 1–2 cm, and 2–5 cm, respectively; f and b refer to fines and bulk sediment particle sizes (see text); Signif, significance at $P < 0.05$, with significant differences shown by different letters by magnetic-property group within a column; MS, magnetic susceptibility in $\text{m}^3 \text{kg}^{-1}$; IRM, isothermal remanent magnetization in $\text{Am}^2 \text{kg}^{-1}$; HIRM, “hard” isothermal remanent magnetization in $\text{Am}^2 \text{kg}^{-1}$ [King and Channell, 1991]; S, S parameter [Thompson and Oldfield, 1986].

analyses (references in Table 1). These analyses reveal two components of sediment in the isolated settings: (1) a component derived by physical weathering of local bedrock; and (2) a component that cannot have been derived from local bedrock because of greatly different mineralogy, Sr isotopic composition, and particle-size distribution. The silt-and-clay size fractions of nearly all pothole sediments contain elevated abundances of fines in the range 2–20 μm , consistent with far-traveled dust. In addition, field observations and petrologic results serve to reject the possibility that residual concentration of strongly magnetic minerals has resulted from weathering. The possibility that the magnetic contrasts are related to pedogenic development of iron oxides is rejected on the basis of (1) absence of soil development in the 0–10 cm depths; (2) highly correlated MS and IRM ($R^2 > 0.96$ for

group 1, 2, and 3 samples), indicating that particles sufficiently large to have permanent magnetization dominate MS; and (3) low values of FDMS from this depth interval [see Dearing *et al.*, 1996]. Group 1 fines had an average FDMS = 2.5% (standard deviation = 0.3, $N = 14$), and group 1 bulk sediments had an average FDMS = 2.0% (standard deviation = 1.8, $N = 99$).

3.3. Causes for Variations in Dust Concentrations in Isolated Settings

[20] Within- and among-site variations in magnetic properties of sediments in isolated settings (Figure 4 and Table 2) do not arise primarily from dilution of atmospheric dust by coarse-grained sediment derived from locally weathered bedrock. Bulk sediments from the BSC and underlying deposits at

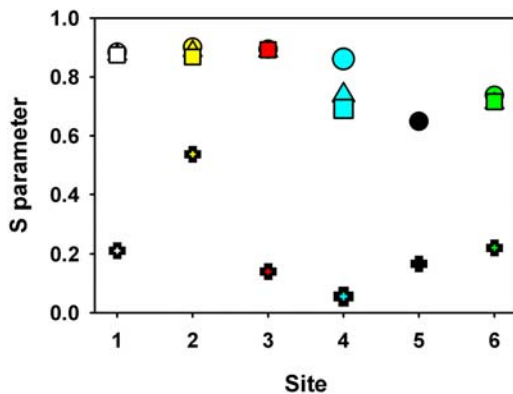


Figure 5. Plot of S-parameter values for sediments and associated reddish sedimentary rocks (hematite-bearing; plus symbols). For each site, three values are plotted for surficial sediment. Circles denote top-most sample (0–1 cm depth); triangles, intermediate depths (1–3 cm); squares, bottom sample (typically 3–5 cm); crosses, bedrock. Sites: 1 represents 493; 2, 29; 3, 55; 4, 54; 5, 7U-2; 6, 7U-8 (see Figure 1).

group-1 sites have the same average silt content (23%) and similar sand content (67% and 60%, respectively). At group-2 sites, sediment at all depths is also dominated by sand (>50%), and textural trends with sample depth are lacking [Goldstein *et al.*, 2008].

[21] Magnetic-property differences, rather, are strongly related to regional location and may be related to time (within-site vertical extent). Magnetite concentrations based on MS and IRM values in both fine-fraction and bulk samples are significantly higher ($P < 0.001$) in the sites from the eastern Mojave Desert than in sites on the Colorado Plateau (Figure 4 and Table 2). Goldstein *et al.* [2008] showed that IRM values for group-2 sites declined systematically from west to east. As with magnetite, hematite concentrations inferred from HIRM values decline from west to east, except in the central part of the Colorado Plateau, where relatively elevated HIRM likely reflects nearby dust inputs and (or) detritus locally derived from physically weathered hematite-bearing bedrock that is common in this area [Goldstein *et al.*, 2008]. The spatial and temporal patterns in magnetite concentration are tracked by variations in chemically immobile elements that reside in high-density minerals. For example, Ti concentrations in group-2 samples diminish west-to-east and mimic declines in IRM [Goldstein *et al.*, 2008].

[22] The new magnetic results on group-1 fines enable tests of previous suggestions [Reynolds *et al.*, 2001a] that aeolian magnetite inputs to these

surficial deposits have increased over time. For all sample sets (fines and bulk sediment), MS and IRM are highest at the top depth interval and diminish systematically with increasing depth. As shown in Table 2, such differences at the three depth intervals are not significant at $P < 0.05$, except for higher IRM in Mojave top-interval fines compared with those in the bottom interval. Nevertheless, IRM for Colorado Plateau top-interval fines (mean, $4.59 \times 10^{-3} \text{ Am}^2 \text{ kg}^{-1}$) is higher (significant at $P = 0.14$) than underlying sediments (mean, $3.66 \times 10^{-3} \text{ Am}^2 \text{ kg}^{-1}$). Similarly, IRM for Mojave fines in the top layer (mean, $1.43 \times 10^{-2} \text{ Am}^2 \text{ kg}^{-1}$) is higher (significant at $P = 0.12$) than underlying sediments (mean, $1.12 \times 10^{-2} \text{ Am}^2 \text{ kg}^{-1}$). The very small differences among S-parameter values for these samples sets (Table 2) are consistent with increasing inputs of magnetite, relative to hematite, over time. The interpretation of increasing magnetite deposition during the past century is consistent with results from subalpine lakes in the Uinta Mountains in northeastern Utah (about 60–150 km east of Salt Lake City (Figure 1)). In two lacustrine records that span the past several thousand years, concentrations of silt-size and titanium-bearing magnetite increase by a factor of about six in sediments deposited since AD1870. Such magnetite is lacking in the Precambrian sedimentary bedrock in the catchments for these lakes and across the mountain range, and it is interpreted

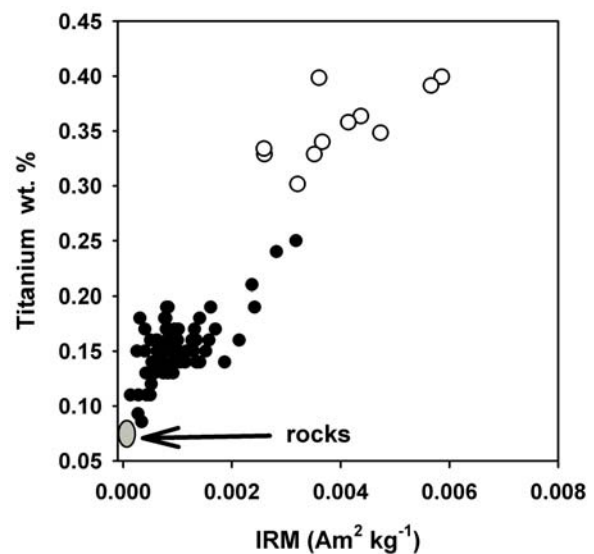


Figure 6. Plot of isothermal remanent magnetization against titanium in weight per cent determined using X-ray fluorescence. Open (closed) symbols, fine-fraction (coarse-fraction) sediments in group-1; oval encompasses results from associated bedrock samples. For the sediments, $R^2 = 0.83$.

Table 3. Summary of Results From Hillslope Transects Comparing Isothermal Remanent Magnetization, Nutrients, Estimated Dust Concentrations, and Fines^a

Site-Position	IRM	Nutrients	Dust (%)	Fines (%)
NG-1	2.64E-04	1.8	1.8	18.2
NG-2	8.27E-04	2.4	6.4	23.3
NG-3	1.00E-03	2.5	7.8	23.0
NG-4	9.39E-04	2.5	7.3	27.0
NG-5	1.15E-03	3.2	8.3	33.2
NG-6	1.40E-03	3.6	11.0	27.2
NG-7	1.98E-03	4.4	15.7	39.1
NG-8	1.69E-03	4.1	13.3	32.8
NG-9	1.94E-03	4.3	15.4	32.0
NG-10	2.15E-03	4.6	17.1	32.5
NG-11	2.20E-03	4.3	17.5	37.3
NG-12	2.14E-03	4.5	17.0	36.9
HG-1-1	9.68E-04	2.1	6.8	17.4
HG-1-1	9.68E-04	3.1	6.8	17.4
HG-1-2	6.66E-04	2.6	4.6	18.8
HG-1-3	7.66E-04	2.9	5.3	12.8
HG-1-4	9.35E-04	3.1	6.6	18.3
HG-1-5	9.79E-04	3.5	6.9	14.4
HG-1-6	1.50E-03	5.0	10.7	25.1
HG-2-1	1.57E-04	2.9	0.9	16.6
HG-2-2	1.12E-04	3.1	0.5	4.2
HG-2-3	1.57E-04	3.4	0.9	6.2
HG-2-4	1.87E-04	3.5	1.1	25.9
HG-2-5	1.76E-04	3.2	1.0	2.9
HG-2-6	2.52E-04	3.8	1.6	13.7
HG-2-7	1.98E-04	3.6	1.2	18.5
HG-2-8	3.29E-04	3.9	2.1	3.9
HG-2-9	3.03E-04	4.0	1.9	35.2
HG-2-10	4.45E-04	4.8	3.0	34.1
HG-2-11	3.80E-04	4.5	2.5	21.9
HG-3-1	4.03E-04	3.2	2.2	10.1
HG-3-2	6.09E-04	3.6	3.5	13.5
HG-3-3	7.17E-04	3.4	4.2	11.1
HG-3-4	6.99E-04	3.6	4.1	15.2
HG-3-5	6.83E-04	3.6	4.0	12.4
HG-3-6	7.33E-04	3.9	4.3	14.8
HG-3-7	8.09E-04	3.8	4.8	13.8
HG-3-8	7.85E-04	3.7	4.7	17.7
HG-3-9	8.37E-04	4.0	5.0	20.4
HG-3-10	7.22E-04	4.0	4.3	13.2
HG-3-11	1.26E-03	5.0	7.8	22.5

^aSite-position, hillslope site and position in transect from top (1) to bottom (highest number); IRM, isothermal remanent magnetization in Am² kg⁻¹; Nutrients, nutrient index, sum of normalized elemental abundances for K, Na, P, Mn, and Zn, as described in text; Dust, dust concentration based on IRM, as discussed in text; Fines, silt-plus-clay contents in vol. per cent measured using laser-diffraction methods.

to have been introduced as far-traveled aeolian dust [Reynolds *et al.*, 2010].

3.4. Magnetic Properties of Hillslope Sediments: Estimates of Dust Concentrations

[23] Magnetic, chemical, and textural properties of hillslope sediments (group 3) change downslope.

Isothermal remanent magnetization in the NG transect increases overall downslope by a factor of 8 along with increasing fines (Table 3). As with isolated sediments, IRM and MS values of hillslope samples are much higher than those for nearby bedrock. Hillslope sediments contain the same types of magnetic minerals as observed in isolated sediments and are similarly interpreted to represent far-traveled atmospheric dust. Winothing by wind has produced sand-dominated deposits in the upper parts of the hillslope at NG transect, whereas sorting by rainfall-runoff has concentrated fines downslope to as much as 40%. In this way, fine-grained aeolian magnetite that falls evenly across slopes is concentrated downslope.

[24] Isothermal remanent magnetization of surficial sediment, rock, and modern dust can be used to estimate the amount of far-traveled dust in the hillslope deposits. As described by Reynolds *et al.* [2006a], the mass fraction of dust (dustf) in each sample is calculated by a binary mixing relation [Albarède, 1995], in which the IRM of the dust and rock components (IRM_{dust} and IRM_{rock}, respectively) and mixture concentrations (IRM_{sed}; IRM of the sediment sample at a transect position) are known:

$$\text{dustf} = (\text{IRM}_{\text{sed}} - \text{IRM}_{\text{rock}}) / (\text{IRM}_{\text{dust}} - \text{IRM}_{\text{rock}}). \quad (1)$$

At NG transect, the value for IRM_{rock} ($3.87 \times 10^{-5} \text{ Am}^2 \text{ kg}^{-1}$) was the mean of 19 samples of Cedar Mesa Sandstone in the region, and IRM_{dust} ($1.24 \times 10^{-2} \text{ Am}^2 \text{ kg}^{-1}$ on sand-free and organic matter-free bases) was measured on modern dust that was collected in 2-m high traps over a six-month period near the middle of the hillslope. The IRM values of sediment ranged from 2.64×10^{-4} to $2.14 \times 10^{-3} \text{ Am}^2 \text{ kg}^{-1}$ from the highest to lowest slope positions. These values respectively corresponded with 2 to 18% dust in the bulk sediment (Figure 7).

[25] For transects HG-1 [Reynolds *et al.*, 2006a] and HG-2, the IRM value used to represent rock was the same value as that for NG transect, because all sites have the Permian Cedar Mesa Sandstone in common. The IRM for dust ($1.37 \times 10^{-2} \text{ Am}^2 \text{ kg}^{-1}$) at both transects was taken from a dust-collection site, located nearly equidistant (~3.5 km) between the two transects, using identical methods as at site NG. For site HG-3, the average rock-IRM value ($6.63 \times 10^{-5} \text{ Am}^2 \text{ kg}^{-1}$) was determined from 15 samples of Jurassic Navajo Sandstone exposed above the hillslope, and the dust-IRM value ($1.54 \times 10^{-2} \text{ Am}^2 \text{ kg}^{-1}$) was from dust collected over a

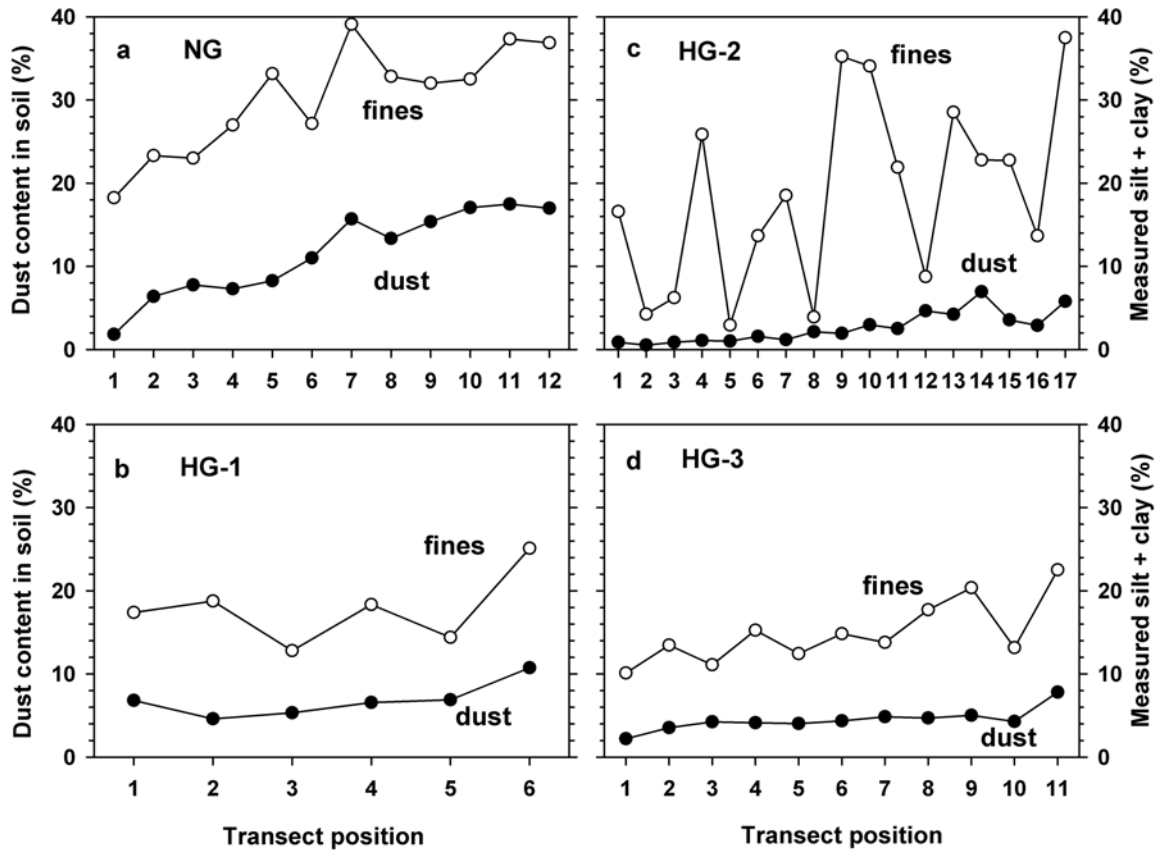


Figure 7. Plots of the abundances of aeolian dust (closed symbols) and measured fines (silt-plus-clay fractions (open symbols)) with position in the transect (sample numbers increase downslope) at (a) site NG, (b) site HG-1, (c) site HG-2, and (d) site HG-3. Figures 7a and 7b are from Reynolds *et al.* [2006a].

six-month period at a location about 10 km from site HG-3. The dust-IRM values represent only three samples but are considered reasonable for estimating dust content in soil. First, the three values are similar, as expected for a large component of time-integrated, well-mixed, and far-traveled dust. Second, the study region that encompasses the four transect localities lacks dominant local dust sources that would differentially influence the three dust-collection sites.

[26] Compared with undisturbed grassland sediment, sediment in disturbed grasslands have generally lower values of IRM that translate into lower concentrations of dust (Figure 7 and Table 3), and these samples also have relatively low concentration of fines (Figures 7 and 8 and Table 3). At site HG-1, dust mostly increases downslope, but the amounts of fines are variable and lack spatial trend. At site HG-2, dust content also generally increases downslope, whereas the fines show extremely large variation associated with an uneven surface of small coppice dunes and intervening swales created

by aeolian activity. The pattern and topographic expressions of these aeolian features, along with the presence of immature cyanobacterial BSC across most of the sampled area, suggest their recent formation, likely within the past approximately 100 years. The dust concentrations at HG-2 apparently represent partial or incipient recovery of nutrient status after disturbance. At site HG-3, sediments show a systematic increase in dust (about 2–8%) and overall downslope increase in fines (10–23%). In summary, the amounts of dust estimated from magnetic measurements show nearly systematic downslope increases over most of the length of each transect, despite different patterns and trends in the amount of fines at the disturbed settings (Figures 7 and 8).

[27] Results from HG-3 greatly strengthen previous, preliminary concepts [Reynolds *et al.*, 2006a] about geomorphic controls on the distribution of dust-derived nutrients on dryland surfaces. The prior results were based on the NG and HG-1 localities at nearly identical elevation, in close

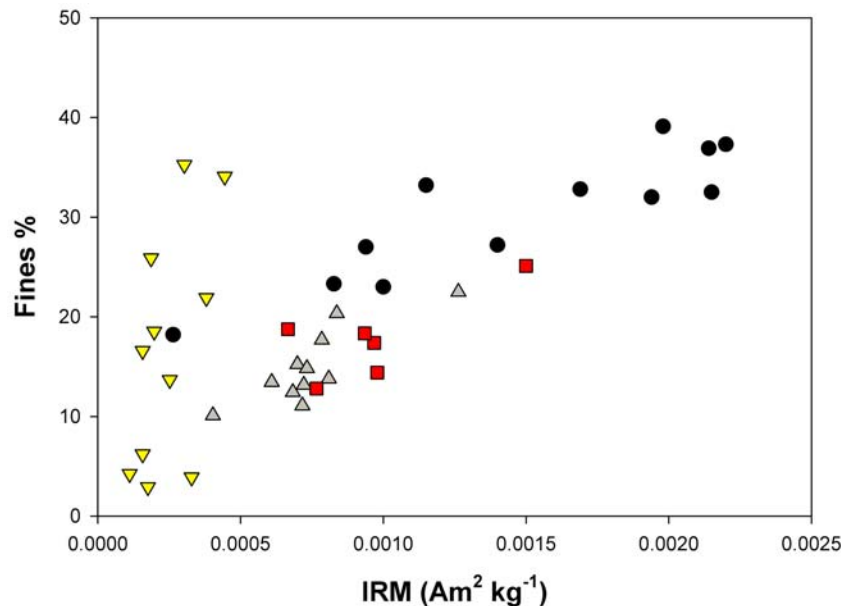


Figure 8. Plots of fines (silt-plus-clay fractions) against isothermal remanent magnetization (IRM) for hillslope transect samples. Solid circles, site NG; squares, site HG-1; inverted triangles, site HG-2; triangles, HG-3.

proximity, and having identical bedrock (Cedar Mesa Sandstone that contains interbedded silty arkosic sandstone). These similarities provided necessary conditions to provide a test for the effects of past disturbance. In addition to sitting in a cooler and wetter environment than at the NG and HG-1 settings, site HG-3 is on a different bedrock substrate, the Navajo Sandstone, having different mineralogy and texture. Compared with settings in the Cedar Mesa Sandstone, sediments derived from the Navajo Sandstone at HG-3 contain little locally derived calcite and hematite, and they contain coarser sand. The results from HG-3 expand the scope of previous conclusions, based on one type of geologic and climatic setting, by representing different and more extensive settings (in space and elevation) underlain by Navajo Sandstone.

3.5. Dust and Nutrients

[28] The contribution of dust to soil nutrients can be elucidated from the associations between elemental abundances and dust concentrations estimated from IRM values. Potential plant nutrients were determined from concentrations of K, Na, P, Mn, and Zn in each sample measured by ICP elemental analyses (methods and data described by Goldstein *et al.* [2005, 2007]). Magnesium was not used because some of it is likely associated with rock-derived calcite at many sites, and Fe was not included because of its highly variable occurrence in bedrock related to hematite. The nutrient index

was calculated in the following ways. For group 2 samples, individual elements were averaged by depth categories for all sites and then a given elemental concentration in each sample in a depth category was normalized to the highest average for that element. The nutrient index of each sample was determined by summing the normalized values of each of the nutrient elements. For group 3 samples (all from the upper 10 cm), the value for each element in each sample was normalized to the maximum value for that element in the entire transect. The normalized values were summed within each sample to yield the nutrient index for that sample.

[29] The IRM values for sediment fines in group-2 sites show positive correlation ($R^2 = 0.54$; all depths combined) with potential plant nutrients (Figure 9). This result reveals that higher concentrations of magnetite-bearing dust are associated with higher amounts of potential nutrients, and it thus suggests that magnetic measures for magnetite can provide rough indications of soil fertility (as well as surface water-holding capacity) in these kinds of settings. The large variability is not surprising considering that the magnetite-bearing dust represents nearly direct fallout at these isolated sites with likely variable degrees of subsequent bioturbation.

[30] At all hillslope sites, IRM values and potential nutrients strongly correlate (Figure 10). The tight relation between IRM (mostly from magnetite and

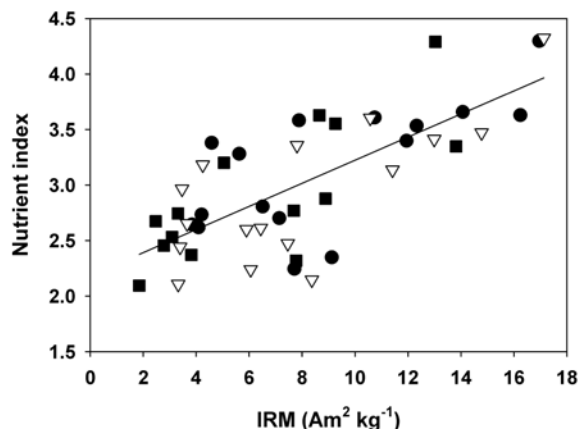


Figure 9. Plots of nutrient index against isothermal remanent magnetization (IRM) for group-2 samples. The nutrient index is the sum of normalized abundances of K, Na, P, Mn, and Zn. Solid circles, 0–1-cm depths; inverted triangles, 1–2-cm depths; squares, 2–5-cm depths. Regression line gives $R^2 = 0.54$.

a proxy for dust) and relative increases in nutrients reflects particle sorting to segregate preferentially the fine-silt fraction that carries most of the dust. The highest IRM value at each of sites HG-1 and -3 represents relatively fine-grained sediment in a swale at the lowest elevation in each transect. Correspondence between IRM and nutrients (Figure 10) is much stronger than between IRM and fines (silt plus clay (Figure 8)) contents. This comparison

underscores the condition that coarse silt does not contribute nutrients to the extent as do fine silt sizes ($<20 \mu\text{m}$). Differences in slopes of the regression line fits are not important because the index represents relative abundances. The important result is that increasing IRM from dust is linked with increasing soil nutrients. Using an approach linking IRM to elemental concentrations, *Reynolds et al.* [2006a] estimated that mineral dust provided 30–90% of the potential plant nutrients in the NG sediments and 20–70% of the nutrients in the HG-1 sediments.

3.6. Magnetic Evidence for Wind-Erosion Depletion of Nutrients

[31] The much higher range of IRM values at the undisturbed site (NG) indicates that more dust currently resides in NG soil than in soil at the other sites. This observation led to the interpretation that historically grazed, disturbed surfaces with broken BSC preferentially lost their magnetite and nutrients as a result of higher degrees of wind erosion [Neff *et al.*, 2005; Reynolds *et al.*, 2006a]. This interpretation has since been supported by analysis of a 10-year monitoring record of aeolian sediment transport and wind erosion at NG and at three nearby sites that have similar disturbance histories to sites HG-1, -2, and -3 [Belnap *et al.*, 2009]. This interpretation is further strengthened by investiga-

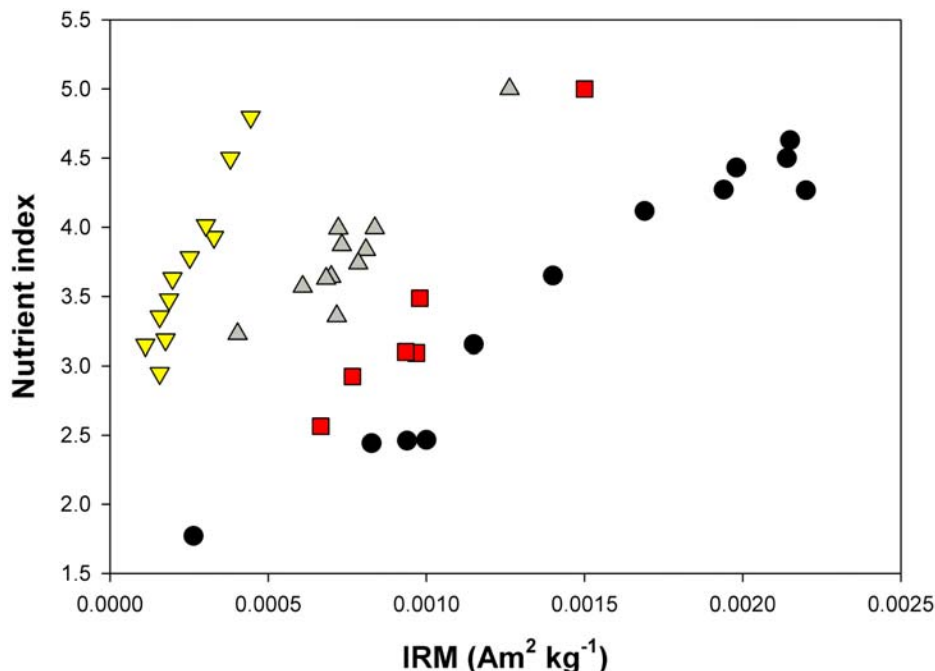


Figure 10. Plots of nutrient index against isothermal remanent magnetization (IRM) for group-3 samples. The nutrient index as for Figure 9 and symbols as for Figure 8.

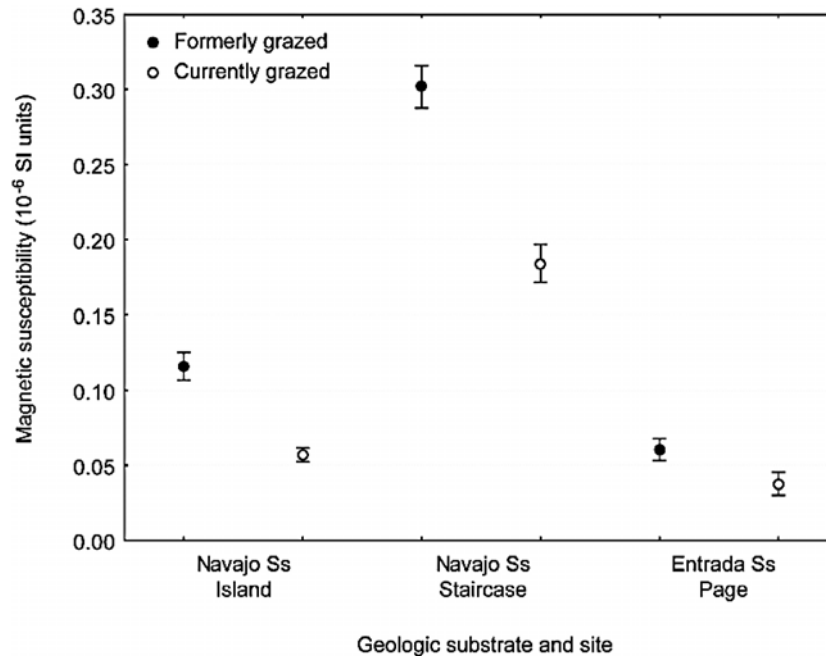


Figure 11. Mean field measurements of MS (± 95 percent CI) for formerly grazed (closed symbols) and currently grazed (open symbols) areas at two sites with soils derived from Navajo Sandstone and one site with soils derived from Entrada Sandstone. For all three sites, t tests indicate that means for formerly and currently grazed areas are significantly different (Island, $n = 30$ formerly grazed and 41 currently grazed measurements, $df = 69$, $t = 12.59$, $p < 0.0001$; Staircase, $n = 27$ formerly grazed and 27 currently grazed measurements, $df = 52$, $t = 12.78$, $p < 0.0001$; Page, $n = 10$ formerly grazed and 10 currently grazed measurements, $df = 18$, $t = 4.85$, $p < 0.001$).

tions of landscape conditions (soil organic carbon and nitrogen, laboratory measurements of MS, and texture) at currently grazed surfaces and at never-grazed surfaces on the Colorado Plateau [Fernandez *et al.*, 2008]. In comparisons between grazed and never-grazed surfaces, paired by bedrock type, the grazed surfaces showed evidence of wind-erosion depletion of nutrients, magnetite, and fines.

4. Applications Using Field Instruments

4.1. Evidence for Accumulation and Erosional Loss of Dust

[32] In sandstone-dominated settings, field measurements of MS in formerly grazed and currently grazed sites are consistent with laboratory measurements described above where regimes of soil-surface disturbance have differed long enough for detectable MS patterns to emerge. At the Island site, mean MS in a grassland rested from livestock use for 30 years was twice the mean that was measured in a comparable currently grazed grassland (Figure 11). Similarly at the Staircase site, mean MS in a shrubland rested from grazing for about 39 years was 1.6 times greater than that measured in the adjacent currently grazed shrub-

land. Mean MS at the Page site also was 1.6 times greater in the shrubland rested for 40 years than in the adjacent grazed shrubland (Figure 11). In each case, differences are interpreted as the net effects of the post-grazing accumulation of dust at formerly grazed sites as well as chronic depletion and lack of accumulation of soil fines at currently grazed sites due to frequent surface disturbance by livestock.

4.2. Invasive Plant Patterns in Relation to Abundance of Aeolian Magnetite

[33] Observed associations between laboratory measurements of IRM and rates of establishment and growth of the invasive annual grass *Bromus tectorum* in sandstone-derived soils of CNP are attributable to the positive correlation between magnetite abundance and silt and clay fractions which control water-holding capacity and nutrient bioavailability at the soil surface [Miller *et al.*, 2006]. These associations were subsequently supported by field measurements of MS at the NG site in CNP (Figure 12). There we found a curvilinear relation between field MS and the frequency (percent occurrence) of *Bromus* in 1-m² quadrats placed along transects traversing long-term study plots.

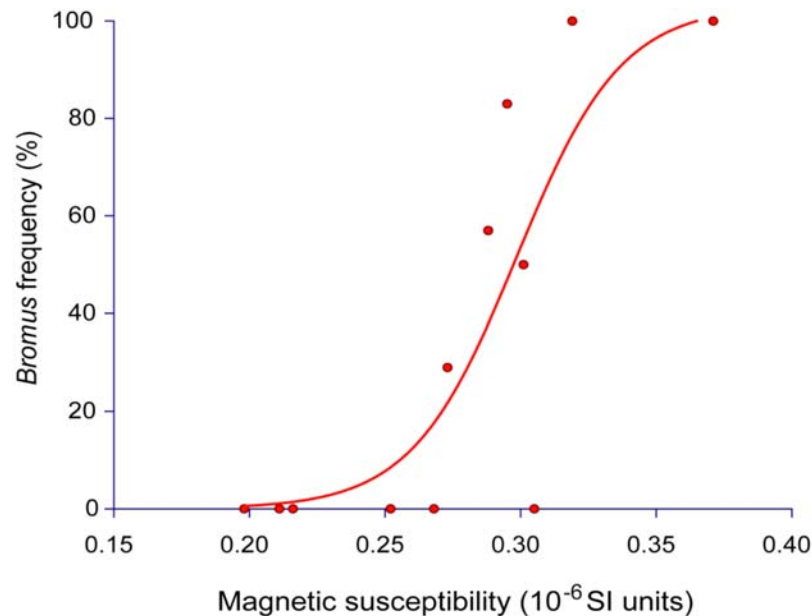


Figure 12. Frequency (percent occurrence in 1-m² quadrats) of the invasive exotic grass *Bromus tectorum* as a function of field magnetic susceptibility measurements in plots at the NG site. Fitted curve is a 3-parameter logistic model ($R^2 = 0.67$).

[34] This curvilinear relation suggests a threshold response of *Bromus* establishment to increasing levels of soil fines through effects on moisture availability to seeds at or near the soil surface. The NG site in CNP may represent an ideal setting for detecting such a response because of (1) sandy soils and (2) the lack of surface disturbance that would otherwise result in seed burial and improved soil-moisture conditions relative to those experienced by seeds on the soil surface [e.g., *Evans and Young, 1972*]. In dryland ecosystems, biological processes such as seed germination and nutrient cycling are recognized for exhibiting threshold responses to temporal pulses in water availability triggered by precipitation events [*Noy-Meir, 1973; Beatley, 1974; Schwinning et al., 2004*]. Soil-surface heterogeneity also is known to affect the dynamics of seedling establishment [*Maestre et al., 2003*]. Therefore, the threshold concept should be equally applicable to spatial patterns in soil resources. The relation between dust content (field MS) and *Bromus* occurrence also suggests that chronic wind erosion and depletion of soil fines in frequently disturbed settings may diminish the suitability of sandy soils for *Bromus* in some cases.

5. Discussion

[35] Dust has been identified in soils and surficial deposits from particle-size analysis; geochemistry

of major, minor, and trace elements; silicate and clay mineralogy, and isotopic studies [*Marchand, 1970; Jackson et al., 1971; McFadden et al., 1987; Wells et al., 1987; Reheis et al., 1995; McDonald et al., 1995; Muhs et al., 2007, 2008*]. Importantly, far-traveled dust is recognized as a source of nutrients in many terrestrial ecosystems [*Swap et al., 1992; Chadwick et al., 1999; Vitousek et al., 1999; Field et al., 2010*]. Moreover, a large body of literature has documented the influences of far-traveled atmospheric mineral dust in the development of dryland soils and landforms [e.g., *Wells et al., 1987; McFadden et al., 1987*]. Dust falls evenly on landscapes, but slope wash processes in deserts can transport modern dust to lower elevations across hillslopes [*Verrecchia et al., 1995; Kidron and Yair, 1997; Shachak and Lovett, 1998*]. On Lanzarote (Canary Islands), Late Quaternary Saharan dust has been redistributed from highlands into valleys by colluvial geomorphic processes, such that valley-fill deposits can be interpreted as a paleoclimatic archive from dust-fall history [*von Suchodoletz et al., 2009*].

[36] We demonstrate here that environmental magnetism can be used to identify recently deposited dust on surfaces that have undergone little modification over at least a century and on topographically uneven terrain where dust is redistributed by geomorphic processes. In the undisturbed NG site, large downslope increases in



magnetite abundance reveal the re-deposition and subsequent concentration of dust along with potential plant nutrients (Figure 10). Human activities on fragile dryland ecosystems, such as grazing by domestic livestock, commonly expose surfaces or break protective soil crust that then promote soil redistribution and alter soil resources, such as fertility and water-holding capacity. Environmental magnetic methods, including use of simple handheld magnetic susceptibility instruments, can be used to recognize such effects of past and ongoing disturbance in some settings. Systematic downslope increases in concentration of aeolian magnetite across previously disturbed hill-slope site HG-2, having greatly varying sand and silt content, imply downslope redistribution and concentration of dust (Figures 7 and 10). The pattern in magnetite occurrence is associated with a similar pattern in potential plant nutrients that apparently reflects partial recovery of nutrient status since grazing ceased there about 35 years ago. Buildup of fines and renewal of nutrient concentrations in these previously grazed settings are likely to be greatly enhanced by trapping of atmospheric dust by BSC [Danin and Ganor, 1991], which require about a century for mature development [Belnap and Eldridge, 2001; Belnap and Warren, 2002]. Even if the surface at HG-2 does not undergo further modification by dune remobilization, recovery to fertility levels as found at the NG site will take many more decades.

[37] Many potential plant nutrients, such as P, Zn, Na, Ca, and K, are not found in magnetite but instead are contained in lithogenic dust that is transported with aeolian magnetite. The clay minerals, smectite and chlorite, have been identified by X-ray diffraction in group-1 surficial sediments but not in associated bedrock, and these aeolian minerals may contribute Na, Ca, Mg, and Mn to soil. Aeolian feldspars, illite, calcite, and dolomite can contribute Ca, Mg, Na, and K. These minerals have been found in both the dust fraction and in some associated bedrock samples, with the exception of dolomite that has not been found in group-1 bedrock samples. Zinc may be derived from feldspar and phyllosilicate minerals (e.g., biotite). Phosphorus contents vary widely and in many different forms in soil across arid and semi-arid ecosystems [Lajtha and Schlesinger, 1988], the sources for which include dust and bedrock [Neff *et al.*, 2006]. Recent studies of alpine and subalpine lakes strongly suggest increased additions of airborne P to ecosystems in the American West within the past approximately 60 years, thereby implicat-

ing sources from agricultural fertilizer [Neff *et al.*, 2008; Reynolds *et al.*, 2010].

[38] The aeolian magnetite described herein does not fingerprint specific dust sources for several reasons. First, fine-grained sediments at dust sources in western North America are commonly mixtures from multiple alluvial sources and older aeolian deposits. Second, atmospheric mixing of dust from many sources occurs during regional windstorms. Nevertheless, the distribution of rock types in the American Southwest suggests that much of the aeolian magnetite and potential plant nutrients at settings on the central Colorado Plateau (inset in Figure 1) were derived from sources west and southwest of the Plateau, as much as several hundreds of kilometers distant. The central Colorado Plateau is remote from large areas of igneous rocks (Figure 1). Although magnetite-bearing intrusive rocks lie within 100 km of this part of the study area, most surficial sediments derived from these rocks do not lie in major upwind areas of our study sites. Moreover, magnetic-property variations in dust-bearing surficial sediments across this study area lack patterns consistent with dust sources related to relatively nearby igneous centers. The patterns of diminishing IRM from the eastern Mojave Desert to the central Colorado Plateau and the similar declines in Ti concentrations in group-2 samples are together consistent with dust sources in the Mojave Desert. Dust plumes that originate in the Mojave Desert and that extend onto the Plateau have been observed in satellite images [Chavez *et al.*, 2002]. These spatial relations and observations strongly imply that much of the aeolian magnetite found in the central Colorado Plateau has been derived from outside the Colorado Plateau and likely also from areas of volcanic rocks at the western margins of the Plateau. A shift in dust sources during the past century is surmised from higher Zr/Ti in the BSC at group-1 sites [Reynolds *et al.*, 2001a] that corresponds with apparent magnetite enrichment. These relations suggest recently increased contributions of dust from felsic igneous rocks, which are common in the Mojave Desert and the Great Basin Deserts, and that have higher Zr/Ti than mafic rocks, which are common at the western margins of the Plateau. The timing and location of these inferred changes in dust sources imply that human disturbances in developing regions remote from the central Colorado Plateau have affected dust fall onto the Plateau. Urbanization, agriculture, surface water diversion, groundwater withdrawal, military activities, driving on dirt roads, and off-road vehicular recreation are among the human actions that have

increased over the past century in the American West and that can generate new dust sources.

6. Conclusions

[39] The magnetic and petrologic results reveal the presence of detrital magnetite as a component of far-traveled aeolian dust deposited in the western U.S. that has been incorporated into surficial deposits derived mostly from local rocks that lack magnetite. The identification of aeolian dust in these settings, in conjunction with geochemical results, demonstrates the importance of dust to the availability of dryland-soil resources (nutrients and water-holding capacity). Conversely, wind erosion of these substrates may result in the preferential loss or redistribution of previously deposited aeolian dust, thereby diminishing soil resources. Environmental magnetic methods can be used to indicate gains and losses of magnetite-bearing aeolian dust at these kinds of settings and to evaluate the factors that render dry landscapes vulnerable to degradation.

[40] The environmental magnetic approach can readily document the presence of magnetite-bearing dust in surficial substrates where deposited on geologic terrain mostly lacking in magnetite. The approach can also be used in regions having widespread magnetite-bearing bedrock [Reheis *et al.*, 2009] and at settings on igneous and metamorphic rocks that contain abundant magnetite. In the central Mojave Desert, for example, widely separated aeolian deposits are found to have closely similar magnetic and chemical properties that reflect mixing of sediments in source regions and the mixing of dust during atmospheric transport, despite large differences in properties of underlying bedrock [Reynolds *et al.*, 2006c]. Rarely, measures of magnetite abundance, such as IRM and MS, were found to have values nearly identical to those of associated bedrock. Under such coincidences, environmental magnetic parameters for magnetic grain size and relative magnetite-ferric oxide content, such as the ratio of anhysteretic remanent magnetization (ARM) to MS, ARM/IRM, and S-ratio, may establish petrologic differences between surficial sediments and bedrock, thus providing evidence for atmospheric dust.

Acknowledgments

[41] We thank Joshua Feinberg, Seth Munson, Ken Kodama, and an anonymous referee for reviews that greatly improved

the manuscript. These studies have benefited from contributions of results and ideas provided by Jayne Belnap, Jason Neff, Daniel Fernandez, Marith Reheis, and Paul Lamothe, as well as from encouragement by Subir Banerjee. We gratefully acknowledge assistance in the laboratory and field by Jiang Xiao, Isla Casteñeda, Yarrow Axford, Rebecca Mann, Gary Skipp, and Eric Fisher. This work was supported by the Global Change Program of the U.S. Geological Survey.

References

- Albarède, F. (1995), *Introduction to Geochemical Modeling*, doi:10.1017/CBO9780511622960, Cambridge Univ. Press, Cambridge, U. K.
- Beatley, J. C. (1974), Phenological events and their environmental triggers in Mojave Desert ecosystems, *Ecology*, *55*, 856–863, doi:10.2307/1934421.
- Belnap, J., and D. Eldridge (2001), Disturbance of biological soil crusts and recovery, in *Biological Soil Crusts: Structure, Function, and Management*, edited by J. Belnap and O. L. Lange, pp. 363–383, Springer, Berlin.
- Belnap, J., and D. A. Gillette (1998), Vulnerability of desert biological soil crusts to wind erosion: The influences of crust development, soil texture, and disturbance, *J. Arid Environ.*, *39*, 133–142, doi:10.1006/jare.1998.0388.
- Belnap, J., and O. L. Lange (Eds.) (2003), *Biological Soil Crusts: Structure, Function, and Management*, Springer, Berlin.
- Belnap, J., and S. L. Phillips (2001), Soil biota in an ungrazed grassland: Response to annual grass (*Bromus tectorum*) invasion, *Ecol. Appl.*, *11*, 1261–1275, doi:10.1890/1051-0761(2001)011[1261:SBIAUG]2.0.CO;2.
- Belnap, J., and S. Warren (2002), Patton's tracks in the Mojave Desert, USA: An ecological legacy, *Arid Land Res. Manage.*, *16*, 245–258, doi:10.1080/153249802760284793.
- Belnap, J., R. L. Reynolds, M. C. Reheis, S. L. Phillips, F. E. Urban, and H. L. Goldstein (2009), Sediment losses and gains across a gradient of livestock grazing and plant invasion in a cool, semi-rid grassland, *Aeolian Res.*, *1*, 27–43, doi:10.1016/j.aeolia.2009.03.001.
- Billingsley, G. H., D. L. Block, and T. J. Felger (2002), Surficial geologic map of the Loop and Druid Arch quadrangles, Canyonlands National Park, Utah, *U.S. Geol. Surv. Misc. Stud. Map, MF-2411*, scale 1:24,000.
- Bloemendal, J., and P. deMenocal (1989), Evidence for a change in the periodicity of tropical climate cycles at 2.4 Myr from whole-core magnetic susceptibility measurements, *Nature*, *342*, 897–900, doi:10.1038/342897a0.
- Chadwick, O. A., L. A. Derry, P. M. Vitousek, B. J. Huebert, and L. O. Hedin (1999), Changing sources of nutrients during four millions years of ecosystem development, *Nature*, *397*, 491–497, doi:10.1038/17276.
- Chavez, P. S., Jr., D. J. MacKinnon, R. L. Reynolds, and M. Velasco (2002), Monitoring dust storms and mapping landscape vulnerability to wind erosion using satellite and ground-based digital images, *Arid Lands Newsl.*, *51*. (Available at <http://ag.arizona.edu/OALS/ALN/aln51/chavez.html>)
- Danin, A., and E. Ganor (1991), Trapping of airborne dust by mosses in the Negev Desert, Israel, *Earth Surf. Processes Landforms*, *16*, 153–162, doi:10.1002/esp.3290160206.
- Dearing, J. A., K. L. Hay, M. J. Baban, A. S. Huddleston, E. M. Wellington, and P. J. Loveland (1996), Magnetic susceptibility of soil: An evaluation of conflicting theories



- using a national data set, *Geophys. J. Int.*, *127*, 728–734, doi:10.1111/j.1365-246X.1996.tb04051.x.
- Evans, M. E., and F. Heller (2003), *Environmental Magnetism: Principles and Applications of Enviromagnetics*, 293 pp., Academic, San Diego, Calif.
- Evans, R. A., and J. A. Young (1972), Microsite requirements for establishment of annual rangeland weeds, *Weed Sci.*, *20*, 350–356.
- Fernandez, D. P., J. C. Neff, and R. L. Reynolds (2008), Biogeochemical and ecological impacts of livestock grazing in semi-arid southeastern Utah, USA, *J. Arid Environ.*, *72*, 777–791, doi:10.1016/j.jaridenv.2007.10.009.
- Field, J. P., J. Belnap, D. D. Breshears, J. C. Neff, G. S. Okin, J. J. Whicker, T. H. Painter, S. Ravi, M. C. Reheis, and R. L. Reynolds (2010), The ecology of dust, *Frontiers Ecol. Environ.*, doi:10.1890/090050, in press.
- Goldstein, H. L., R. L. Reynolds, M. C. Reheis, J. C. Yount, P. Lamothe, H. Roberts, and J. McGeehin (2005), Particle-size, CaCO₃, chemical, magnetic, and age data from surficial deposits in and around Canyonlands National Park, *U.S. Geol. Surv. Open File Rep.*, 2005-1186.
- Goldstein, H. L., R. L. Reynolds, M. C. Reheis, and J. C. Yount (2007), Physical and chemical data from eolian sediment collected along a transect from the Mojave Desert to the Colorado Plateau, *S. Geol. Surv. Open File Rep.*, 2007-1153.
- Goldstein, H. L., R. L. Reynolds, M. C. Reheis, J. C. Yount, and J. C. Neff (2008), Compositional trends in aeolian dust along a transect across the southwestern United States, *J. Geophys. Res.*, *113*, F02S02, doi:10.1029/2007JF000751.
- Haggerty, S. E. (1976), Opaque mineral oxides in terrestrial igneous rocks, in *Oxide Minerals, Short Course Notes Mineral. Soc. of Am.*, vol. 3, edited by D. Rumble, pp. Hg101–Hg300, Mineral. Soc. of Am., Washington, D. C.
- Hunt, A. (1986), The application of mineral magnetic methods to atmospheric aerosol discrimination, *Phys. Earth Planet. Inter.*, *42*, 10–21, doi:10.1016/S0031-9201(86)80005-X.
- Huntoon, P. W., G. H. Billingsley, and W. J. Breed (1982), Geologic map of Canyonlands National Park and vicinity, Utah, Canyonlands Nat. Hist. Assoc., Moab, Utah.
- Jackson, M. L., T. W. M. Levett, J. K. Syers, R. W. Rex, R. N. Clayton, G. D. Sherman, and G. Vehara (1971), Geomorphological relationships of tropospherically derived quartz in the soils of the Hawaiian Islands, *Soil Sci. Soc. Am. Proc.*, *35*, 515–525.
- Kidron, G. J., and A. Yair (1997), Rainfall-runoff relationship over encrusted dune surfaces, Nizzana, western Negev, Israel, *Earth Surf. Processes Landforms*, *22*, 1169–1184, doi:10.1002/(SICI)1096-9837(199712)22:12<1169::AID-ESP812>3.0.CO;2-C.
- Kim, W., S. Doh, and Y. Park (2005), Characterization of anthropogenic magnetic particles in Asian dust using magnetic measurements and electron microscope observations in Seoul, Korea: Preliminary results, *Eos Trans. AGU*, *86*(52), Fall Meet. Suppl., Abstract A11A-0846.
- King, J. W., and J. E. T. Channell (1991), Sedimentary magnetism, environmental magnetism, and magnetostratigraphy, *U.S. Natl. Rep. Int. Union Geod. Geophys. 1987-1990, Rev. Geophys.*, *29*, 358–370.
- Lajtha, K., and W. H. Schlesinger (1988), The biogeochemistry of phosphorus cycling and phosphorus availability along a desert soil chronosequence, *Ecology*, *69*, 24–39, doi:10.2307/1943157.
- Lázaro, F. J., L. Gutiérrez, V. Barrón, and D. Gelado (2008), The speciation of iron in desert dust collected in Gran Canaria (Canary Islands): Combined chemical, magnetic and optical analysis, *Atmos. Environ.*, *42*, 8987–8996, doi:10.1016/j.atmosenv.2008.09.035.
- Liu, Q., A. P. Roberts, J. Torrent, C.-S. Horng, and J. C. Larrasoña (2007), What do the HIRM and S-ratio really measure in environmental magnetism?, *Geochem. Geophys. Geosyst.*, *8*, Q09011, doi:10.1029/2007GC001717.
- Locke, G., and K. K. Bertine (1986), Magnetite in sediments as an indicator of coal combustion, *Appl. Geochem.*, *1*, 345–356, doi:10.1016/0883-2927(86)90020-X.
- Maestre, F. T., J. Cortina, S. Bautista, J. Bellot, and R. Vallejo (2003), Small-scale environmental heterogeneity and spatio-temporal dynamics of seedling establishment in a semiarid degraded ecosystem, *Ecosystems*, *6*, 630–643, doi:10.1007/s10021-002-0222-5.
- Maher, B. A. (2009), Rain and dust: Magnetic records of climate and pollution, *Elements*, *5*, 229–234, doi:10.2113/gselements.5.4.229.
- Maher, B. A., and R. Thompson (1999), *Quaternary Climates, Environments, and Magnetism*, doi:10.1017/CBO9780511535635, Cambridge Univ. Press, Cambridge, U. K.
- Maher, B. A., A. Alekseev, and T. Alekseeva (2003), Magnetic mineralogy of soils across the Russian Steppe: Climatic dependence of pedogenic magnetite formation, *Palaeogeogr. Palaeoclimatol. Palaeoecol.*, *201*(3–4), 321–341, doi:10.1016/S0031-0182(03)00618-7.
- Maher, B. A., T. J. Mutch, and D. Cunningham (2009), Magnetic and geochemical characteristics of Gobi Desert surface sediments: Implications for provenance of the Chinese Loess Plateau, *Geology*, *37*(3), 279–282, doi:10.1130/G25293A.1.
- Marchand, D. E. (1970), Soil contamination in the White Mountains, eastern California, *Geol. Soc. Am. Bull.*, *81*, 2497–2506, doi:10.1130/0016-7606(1970)81[2497:SCITWM]2.0.CO;2.
- McDonald, E. V., L. D. McFadden, and S. G. Wells (1995), The relative influences of climate change, desert dust, and lithologic control on soil-geomorphic processes on alluvial fans, Mojave Desert, California: Summary of results, in *Ancient Surfaces of the East Mojave Desert, San Bernardino County Mus. Assoc. Q.*, vol. 42, edited by R. E. Reynolds and J. Reynolds, pp. 35–42, San Bernardino County Mus. Assoc., Redlands, Calif.
- McFadden, L. D., S. G. Wells, and M. J. Jercinovich (1987), Influences of eolian and pedogenic processes on the origin and evolution of desert pavements, *Geology*, *15*, 504–508, doi:10.1130/0091-7613(1987)15<504:IOEAPP>2.0.CO;2.
- Miller, M. E., J. Belnap, S. W. Beatty, and R. L. Reynolds (2006), Performance of *Bromus tectorum* L. in relation to soil properties, water additions, and chemical amendments in calcareous soils of southeastern Utah, USA, *Plant Soil*, *288*, 1–18, doi:10.1007/s11104-006-0058-4.
- Muhs, D. R., R. L. Reynolds, J. Been, and G. Skipp (2003), Eolian sand transport pathways in the southwestern United States: Importance of the Colorado River and local sources, *Quat. Int.*, *104*, 3–18, doi:10.1016/S1040-6182(02)00131-3.
- Muhs, D. R., J. Budahn, J. M. Prospero, and S. N. Carey (2007), Geochemical evidence for African dust inputs to soils of western Atlantic islands: Barbados, the Bahamas and Florida, *J. Geophys. Res.*, *112*, F02009, doi:10.1029/2005JF000445.
- Muhs, D. R., J. Budahn, D. L. Johnson, M. Reheis, J. Beann, G. Skipp, E. Fisher, and J. A. Jones (2008), Geochemical evidence for airborne dust additions to soils in Channel



- Islands National Park, California, *Geol. Soc. Am. Bull.*, *120*, 106–126, doi:10.1130/B26218.1.
- Neff, J. C., R. L. Reynolds, J. Belnap, and P. Lamothe (2005), Multi-decadal impacts of grazing on soil physical and biogeochemical properties in southeast Utah, *Ecol. Appl.*, *15*, 87–95, doi:10.1890/04-0268.
- Neff, J. C., R. L. Reynolds, R. L. Sanford, D. P. Fernandez, and P. Lamothe (2006), Geologic controls over soil and plant chemistry in southeastern Utah, *Ecosystems*, *9*, 879–893, doi:10.1007/s10021-005-0092-8.
- Neff, J. C., A. P. Ballantyne, G. L. Famer, N. M. Mahowald, J. L. Conroy, C. C. Landry, J. T. Overpeck, T. H. Painter, C. R. Lawrence, and R. L. Reynolds (2008), Increasing eolian dust deposition in the western United States linked to human activity, *Nat. Geosci.*, *1*, 189–195, doi:10.1038/ngeo133.
- Newsome, D., and J. Walden (2000), Mineral magnetic evidence for heterogeneous sandplain regolith in Western Australia, *J. Arid Environ.*, *45*(2), 139–150, doi:10.1006/jare.2000.0632.
- Noy-Meir, I. (1973), Desert ecosystems: Environment and producers, *Annu. Rev. Ecol. Syst.*, *4*, 25–51, doi:10.1146/annurev.es.04.110173.000325.
- Reed, J. C., Jr., J. O. Wheeler, and B. E. Tucholke (2005), Geologic map of North America—Perspectives and explanation, *Decade of North American Geology*, vol. 3 sheets (74 × 39), scale 1:5,000,000, Geol. Soc. of Am., Boulder, Colo.
- Reheis, M. (2003), Dust deposition in Nevada, California, and Utah, 1984–2002, *U.S. Geol. Surv. Open File Rep.*, *2003-138*. (Available at <http://pubs.usgs.gov/of/2003/ofr-03-138/>)
- Reheis, M. C., J. C. Goodmacher, J. W. Harden, L. D. McFadden, T. K. Rockwell, R. R. Shroba, J. M. Sowers, and E. M. Taylor (1995), Quaternary soils and dust deposition in southern Nevada and California, *Geol. Soc. Am. Bull.*, *107*, 1003–1022, doi:10.1130/0016-7606(1995)107<1003:QSADDI>2.3.CO;2.
- Reheis, M. C., R. L. Reynolds, H. Goldstein, H. M. Roberts, J. C. Yount, Y. Axford, L. S. Cummings, and N. Shearin (2005), Late Quaternary eolian and alluvial response to paleoclimate, Canyonlands, southern Utah, *Geol. Soc. Am. Bull.*, *117*, 1051–1069, doi:10.1130/B25631.1.
- Reheis, M. C., J. R. Budhan, P. L. Lamothe, and R. L. Reynolds (2009), Compositions of modern dust and surface sediments in the desert southwest, USA, *J. Geophys. Res.*, *114*, F01028, doi:10.1029/2008JF001009.
- Reynolds, R. L., J. Belnap, M. C. Reheis, P. Lamothe, N. Mazza, and F. Luiszer (2001a), Eolian dust in Colorado Plateau soils: Nutrient inputs and recent change in source, *Proc. Natl. Acad. Sci. U. S. A.*, *98*, 7123–7127, doi:10.1073/pnas.121094298.
- Reynolds, R. L., D. S. Sweetkind, and Y. Axford (2001b), An inexpensive magnetic mineral separator for fine-grained sediment, *U.S. Geol. Surv. Open File Rep.*, *2001-281*.
- Reynolds, R. L., J. C. Neff, M. C. Reheis, and P. Lamothe (2006a), Atmospheric dust in modern soil on aeolian sandstone, Colorado Plateau (USA): Variation with landscape position and contribution to potential plant nutrients, *Geoderma*, *130*, 108–123, doi:10.1016/j.geoderma.2005.01.012.
- Reynolds, R. L., M. C. Reheis, J. C. Neff, H. Goldstein, and J. C. Yount (2006b), Late Quaternary eolian dust in surficial deposits of a Colorado Plateau grassland: Controls on distribution and ecologic effects, *Catena*, *66*, 251–266, doi:10.1016/j.catena.2006.02.003.
- Reynolds, R. L., M. C. Reheis, J. C. Yount, and P. Lamothe (2006c), Composition of aeolian dust in natural traps on isolated surfaces of the central Mojave Desert (USA)—Insights to mixing, sources, and nutrient inputs, *J. Arid Environ.*, *66*, 42–61, doi:10.1016/j.jaridenv.2005.06.031.
- Reynolds, R. L., J. Mordecai, J. G. Rosenbaum, M. E. Ketterer, M. K. Walsh, and K. Moser (2010), Compositional changes in sediments of subalpine lakes, Uinta Mountains, Utah: Evidence for the effects of human activity on atmospheric dust inputs, *J. Paleolimnol.*, *44*, 161–175, doi:10.1007/s10933-9394-8.
- Schwinning, S., O. E. Sala, M. E. Loik, and J. R. Ehleringer (2004), Thresholds, memory, and seasonality: Understanding pulse dynamics in arid/semi-arid ecosystems, *Oecologia*, *141*, 191–193, doi:10.1007/s00442-004-1683-3.
- Shachak, M., and G. M. Lovett (1998), Atmospheric deposition to a desert ecosystem and its implications for management, *Ecol. Appl.*, *8*, 455–463, doi:10.1890/1051-0761(1998)008[0455:ADTADE]2.0.CO;2.
- Swap, R., M. Garstang, S. Greco, R. Talbot, and P. Kallberg (1992), Saharan dust in the Amazon Basin, *Tellus, Ser. B*, *44*, 133–149.
- Thompson, R., and F. Oldfield (1986), *Environmental Magnetism*, Allen and Unwin, London.
- Verrecchia, E., A. Yair, G. J. Kidron, and K. Verrecchia (1995), Physical properties of the psammophile cryptogamic crust and their consequences to the water regime of sandy soils, north-western Negev Desert, Israel, *J. Arid Environ.*, *29*, 427–437, doi:10.1016/S0140-1963(95)80015-8.
- Vitousek, P. M., M. J. Kennedy, L. A. Derry, and O. A. Chadwick (1999), Weathering versus atmospheric sources of strontium in ecosystems on young volcanic soils, *Oecologia*, *121*, 255–259, doi:10.1007/s004420050927.
- von Suchodoletz, H., D. Fuast, and L. Zöller (2009), Geomorphological investigations of sediment traps on Lanzarote (Canary Islands) as a key for the interpretation of a palaeoclimate archive off NW Africa, *Quat. Int.*, *196*, 44–56, doi:10.1016/j.quaint.2008.03.014.
- Walden, J., K. H. White, S. H. Kilcoyne, and P. M. Bentley (2000), Analyses of iron oxide assemblages within Namib dune sediments using high field remanence measurements (9T) and Mössbauer analysis, *J. Quat. Sci.*, *15*(2), 185–195, doi:10.1002/(SICI)1099-1417(200002)15:2<185::AID-JQS503>3.0.CO;2-5.
- Wells, S. G., L. D. McFadden, and J. C. Dohrenwend (1987), Influence of late Quaternary climatic changes on geomorphic and pedogenic processes on a desert piedmont, eastern Mojave Desert, California, *Quat. Res.*, *27*, 130–146, doi:10.1016/0033-5894(87)90072-X.